



Supplement of

Nitrogen fixation and the diazotroph community in the temperate coastal region of the northwestern North Pacific

T. Shiozaki et al.

Correspondence to: T. Shiozaki (shiozaki@aori.u-tokyo.ac.jp)

The copyright of individual parts of the supplement might differ from the CC-BY 3.0 licence.

Introduction

The supplementary material for this manuscript consists of one table and five figures. The figure captions including methodology are given below.

Fig. S1. Sampling locations for each cruise in the northwestern North Pacific Ocean. Background contours and vectors denote the sea surface temperature (SST) and geostrophic current field during the cruise period. The SST dataset was the daily MODIS level-3 SST with 4-km resolution, and was obtained from the NASA Goddard Space Flight Center (<http://oceancolor.gsfc.nasa.gov/>). Weekly geostrophic current field data with $1/3^{\circ}$ for approximately the same period as the cruise were obtained from the AVISO data server (<ftp://aviso.oceanobs.com>). The gray line during the KK-13-6_Sep cruise indicates the track of Typhoon Man-yi. The flow volume of the Tsushima Water Current is recognized to be largest in summer and makes an anticyclonic eddy on the Pacific side, and is smallest in winter when it does not form the eddy structure (Conlon, 1982; Nishida et al., 2003). During the KT-12-20_Aug, KT-12-27_Oct, KK-13-1_Jun, and KK-13-6_Sep cruises, the anticyclonic eddy was observed on the Pacific side, and the water flowed southward along the coast. The Tsugaru Warm water during the KT-13-2_Jan cruise immediately flowed along the coast after it passed the Tsugaru Strait. Although the southward current subsided at the observation lines during the KT-13-2_Jan cruise, all the water at the surface belonged to the Tsushima Water Current. During the KS-14-2_Mar cruise, the flow from the Tsugaru Strait was weak, and water with a temperature less than 3°C spread to the south of the OT transect line, suggesting that the OT transect line was influenced by the Oyashio water. During the KK-13-6_Sep cruise, a low SST belt was observed

from south to north on the Pacific side. This belt almost corresponded with the typhoon track, and thus was caused by the passage of the typhoon.

Fig. S2. Surface spatial distributions of (a and b) nitrate and (c and d) ammonium concentration [μM] and (e and f) the nitrogen fixation rate [$\text{nmol N L}^{-1} \text{ d}^{-1}$] along the OT and ON transect lines for each cruise.

Fig. S3. Maximum likelihood phylogenetic trees of *nifH* amino acid sequences of Proteobacteria in Cluster I. The recovered sequences in this study are in boldface type. The boldface numbers in parentheses are the number of retrieved clones for each cruise and station. Bootstrap values (>50%) are indicated at branch points. Sequences with an asterisk have >97% similarity at the amino acid level with terrestrial diazotrophs, and with sequences derived from soil, mudflats, and lakes.

Fig. S4. Maximum likelihood phylogenetic trees of *nifH* amino acid sequences of Cyanobacteria in Cluster I. The recovered sequences in this study are in boldface type. The boldface numbers in parentheses are the number of retrieved clones for each cruise and station. Bootstrap values (>50%) are indicated at branch points. Sequences with an asterisk have >97% similarity at the amino acid level with terrestrial diazotrophs.

Fig. S5. Maximum likelihood phylogenetic trees of *nifH* amino acid sequences in Cluster III. The recovered sequences in this study are in boldface type. Boldface numbers in parentheses are the number of retrieved clones for each cruise and station. Bootstrap values (>50%) are indicated at branch points. Sequences with an asterisk

have >97% similarity at the amino acid level with sequences derived from mudflats.

Fig. S6. Surface spatial distributions of (a and b) *Trichodesmium*, (c and d) UYCN-A, (e and f) UCYN-B, and (g and h) γ -24774A11 [$\text{Log}_{10}((\text{copy}+1) \text{ L}^{-1})$] along the OT and ON transect lines for each cruise.

Fig. S7. Vertical profiles of salinity along the OT transect line during the KK-13-6_Sep cruise.

Fig. S8. Vertical profiles of the oxygen concentration [ml L^{-1}] for each cruise.

REFERENCES

- Conlon, D. M.: On the outflow modes of the Tsugaru Warm Current, *La mer*, 20, 60-64, 1982.
- Nishida, Y., Kanomata, I., Tanaka, I., Sato, S., Takahashi, S., and Matsubara, H.: Seasonal and interannual variations of the volume transport through the Tsugaru Strait, *Oceanogr. Japan*, 12(5), 487-499, 2003.

Table S1 Water properties and nitrogen fixation used for Pearson's correlation analysis

Cruise	Station	Latitude	Longitude	Depth	Temperature[°C]	Nitrate [µM]	Ammonium [µM]	Phosphate [µM]	N/P ratio	N ₂ fixation [nmolN L ⁻¹ d ⁻¹]
KT-12-20_Aug	OT1	39.34295	141.9351	0	21.9	0.05	0.22	0.20	0.25	2.84
KT-12-20_Aug	OT4	39.33318	142.1663	0	21.7	<0.02	0.03	<0.01	5.37	10.8
KT-12-20_Aug	OT4	39.33318	142.1663	11	19.5	<0.02	<0.03	<0.01	5.00	12.0
KT-12-20_Aug	OT4	39.33318	142.1663	34	15.8	<0.02	<0.03	<0.01	5.00	1.20
KT-12-20_Aug	OT4	39.33318	142.1663	63	13.2	2.80	<0.03	0.36	9.15	n.d.
KT-12-20_Aug	OT5	39.33357	142.4981	0	23.9	<0.02	<0.03	<0.01	5.00	8.50
KT-12-20_Aug	OT6	39.3318	142.8352	0	24.3	<0.02	<0.03	<0.01	5.00	0.49
KT-12-20_Aug	ON1	38.42083	141.4858	0	22.4	<0.02	0.05	<0.01	7.39	2.82
KT-12-20_Aug	ON4	38.41697	141.7507	0	20.6	<0.02	<0.03	0.08	0.67	3.34
KT-12-20_Aug	ON5	38.41721	142	0	22.3	<0.02	0.02	0.03	1.42	5.02
KT-12-20_Aug	ON5	38.41721	142	9	21.8	<0.02	<0.03	<0.01	5.00	3.79
KT-12-20_Aug	ON5	38.41721	142	34	11.9	0.85	<0.03	0.15	6.10	n.d.
KT-12-20_Aug	ON5	38.41721	142	62	10.1	8.05	<0.03	0.69	11.7	n.d.
KT-12-20_Aug	ON6	38.41782	142.3326	0	22.5	<0.02	0.11	0.05	2.63	7.95
KT-12-20_Aug	ON7	38.41569	142.6659	0	21.0	<0.02	<0.03	0.13	0.39	n.d.
KT-12-27_Oct	OT1	39.34597	141.954	0	20.3	0.11	0.05	0.10	2.42	n.d.
KT-12-27_Oct	OT4	39.33318	142.1663	0	20.0	<0.04	0.08	0.08	1.37	0.45
KT-12-27_Oct	OT4	39.33318	142.1663	31	19.8	0.04	0.05	0.06	1.84	1.80
KT-12-27_Oct	OT4	39.33318	142.1663	62	16.3	3.17	0.05	0.32	11.2	0.30
KT-12-27_Oct	OT5	39.33357	142.4981	0	19.7	<0.04	0.08	0.07	1.70	n.d.
KT-12-27_Oct	OT6	39.3318	142.8352	0	19.8	<0.04	0.10	0.08	1.64	0.33
KT-12-27_Oct	ON1	38.42527	141.4883	0	21.2	0.07	0.10	0.15	1.80	0.59
KT-12-27_Oct	ON4	38.41697	141.7507	0	20.2	<0.04	0.06	0.07	1.49	2.26
KT-12-27_Oct	ON5	38.41721	142	0	20.8	<0.04	0.05	0.06	1.64	n.d.
KT-12-27_Oct	ON5	38.41721	142	32	20.8	0.11	0.05	0.06	3.07	n.d.
KT-12-27_Oct	ON5	38.41721	142	65	13.3	5.77	0.06	0.50	11.7	n.d.
KT-12-27_Oct	ON7	38.41569	142.6659	0	20.3	<0.04	0.62	0.09	7.40	0.72
KT-13-2_Jan	OT1	39.34597	141.954	0	9.8	5.22	0.18	0.47	11.9	n.d.
KT-13-2_Jan	OT4	39.33318	142.1663	0	9.8	6.16	0.16	0.50	12.8	n.d.
KT-13-2_Jan	OT4	39.33318	142.1663	41	9.6	6.11	0.16	0.50	12.7	n.d.
KT-13-2_Jan	OT4	39.33318	142.1663	76	9.4	6.30	0.16	0.52	12.6	n.d.
KT-13-2_Jan	OT5	39.33357	142.4981	0	9.3	6.47	0.15	0.52	12.8	n.d.
KT-13-2_Jan	OT6	39.3318	142.8352	0	9.8	6.16	0.16	0.50	12.8	n.d.
KT-13-2_Jan	ON1	38.42527	141.4883	0	8.8	0.75	0.35	0.27	4.50	n.d.
KT-13-2_Jan	ON4	38.41697	141.7507	0	9.0	6.93	0.14	0.55	13.1	n.d.
KT-13-2_Jan	ON5	38.41721	142	0	8.3	7.95	0.07	0.63	12.8	n.d.
KT-13-2_Jan	ON5	38.41721	142	62	7.3	9.84	0.07	0.80	12.4	n.d.
KT-13-2_Jan	ON5	38.41721	142	119	6.5	12.0	0.06	0.98	12.4	n.d.
KT-13-2_Jan	ON6	38.41782	142.3326	0	9.8	6.01	0.01	0.46	13.1	n.d.
KK-13-1_Jun	OT4	39.33318	142.1663	0	14.6	<0.02	<0.01	<0.01	3.00	0.87
KK-13-1_Jun	OT4	39.33318	142.1663	23	12.7	0.12	0.03	0.02	7.03	0.61
KK-13-1_Jun	OT4	39.33318	142.1663	42	11.7	1.53	0.62	0.18	12.9	1.56
KK-13-1_Jun	OT5	39.3176	142.5002	0	16.4	0.04	0.07	0.02	6.59	n.d.
KK-13-1_Jun	OT6	39.33345	142.8319	0	15.4	<0.02	<0.01	<0.01	3.00	0.86
KK-13-1_Jun	ON1	38.42158	141.4855	0	15.4	<0.02	0.02	<0.01	4.22	3.83
KK-13-1_Jun	ON4	38.41645	141.7497	0	18.5	<0.02	0.03	<0.01	4.84	n.d.
KK-13-1_Jun	ON5	38.41646	142.0007	0	16.8	<0.02	0.10	<0.01	11.8	n.d.
KK-13-1_Jun	ON5	38.41646	142.0007	25	8.9	1.69	0.06	0.28	6.74	n.d.
KK-13-1_Jun	ON5	38.41646	142.0007	44	9.2	5.00	0.05	0.37	13.8	n.d.
KK-13-1_Jun	ON6	38.41773	142.3338	0	14.2	<0.02	0.17	<0.01	18.6	n.d.
KK-13-1_Jun	ON7	38.4167	142.6679	0	19.4	<0.02	0.06	<0.01	7.59	n.d.
KK-13-1_Jun	ON8	38.41681	143.0004	0	19.4	<0.02	0.03	<0.01	5.03	n.d.
KK-13-6_Sep	OT1	39.34126	141.9318	0	22.5	22.5	1.41	0.33	72.2	n.d.
KK-13-6_Sep	OT4	39.33318	142.1663	0	22.8	0.30	<0.01	0.04	9.54	0.76
KK-13-6_Sep	OT4	39.33318	142.1663	38	20.4	1.16	<0.01	0.10	15.3	n.d.
KK-13-6_Sep	OT4	39.33318	142.1663	72	15.5	4.32	0.10	0.32	13.9	n.d.
KK-13-6_Sep	OT5	39.3176	142.5002	0	19.1	0.16	<0.01	0.12	1.67	2.18
KK-13-6_Sep	OT6	39.33345	142.8319	0	20.7	0.23	<0.01	0.05	5.35	0.75
KK-13-6_Sep	ON4	38.41645	141.7497	0	22.3	0.04	<0.01	0.03	1.95	0.64
KK-13-6_Sep	ON5	38.41646	142.0007	0	20.0	<0.02	<0.01	0.08	0.36	0.77
KK-13-6_Sep	ON6	38.41773	142.3338	0	20.3	0.03	<0.01	0.13	0.49	0.45
KK-13-6_Sep	ON7	38.4167	142.6679	0	23.4	0.08	<0.01	0.02	5.88	13.3
KS-14-2_Mar	OT4	39.33318	142.1663	0	2.1	11.8	0.19	1.09	11.2	n.d.
KS-14-2_Mar	OT4	39.33318	142.1663	14	2.1	12.6	0.30	1.14	11.7	n.d.
KS-14-2_Mar	OT4	39.33318	142.1663	26	2.1	13.3	0.22	1.19	11.7	n.d.
KS-14-2_Mar	OT5	39.3176	142.5002	0	1.5	15.1	0.08	1.35	11.5	n.d.
KS-14-2_Mar	OT6	39.33345	142.8319	0	2.4	11.3	0.11	1.13	10.3	n.d.
KS-14-2_Mar	ON4	38.41645	141.7497	0	7.4	10.1	0.08	0.77	13.6	n.d.
KS-14-2_Mar	ON5	38.41646	142.0007	0	7.3	10.0	0.07	0.75	13.8	n.d.
KS-14-2_Mar	ON5	38.41646	142.0007	25	7.3	9.98	0.02	0.74	13.7	n.d.
KS-14-2_Mar	ON5	38.41646	142.0007	65	7.3	10.1	0.04	0.75	13.7	n.d.
KS-14-2_Mar	ON6	38.41773	142.3338	0	7.6	9.88	0.04	0.74	13.7	n.d.
KS-14-2_Mar	ON7	38.4167	142.6679	0	8.1	9.04	0.03	0.66	14.0	n.d.

n.d. = not detected

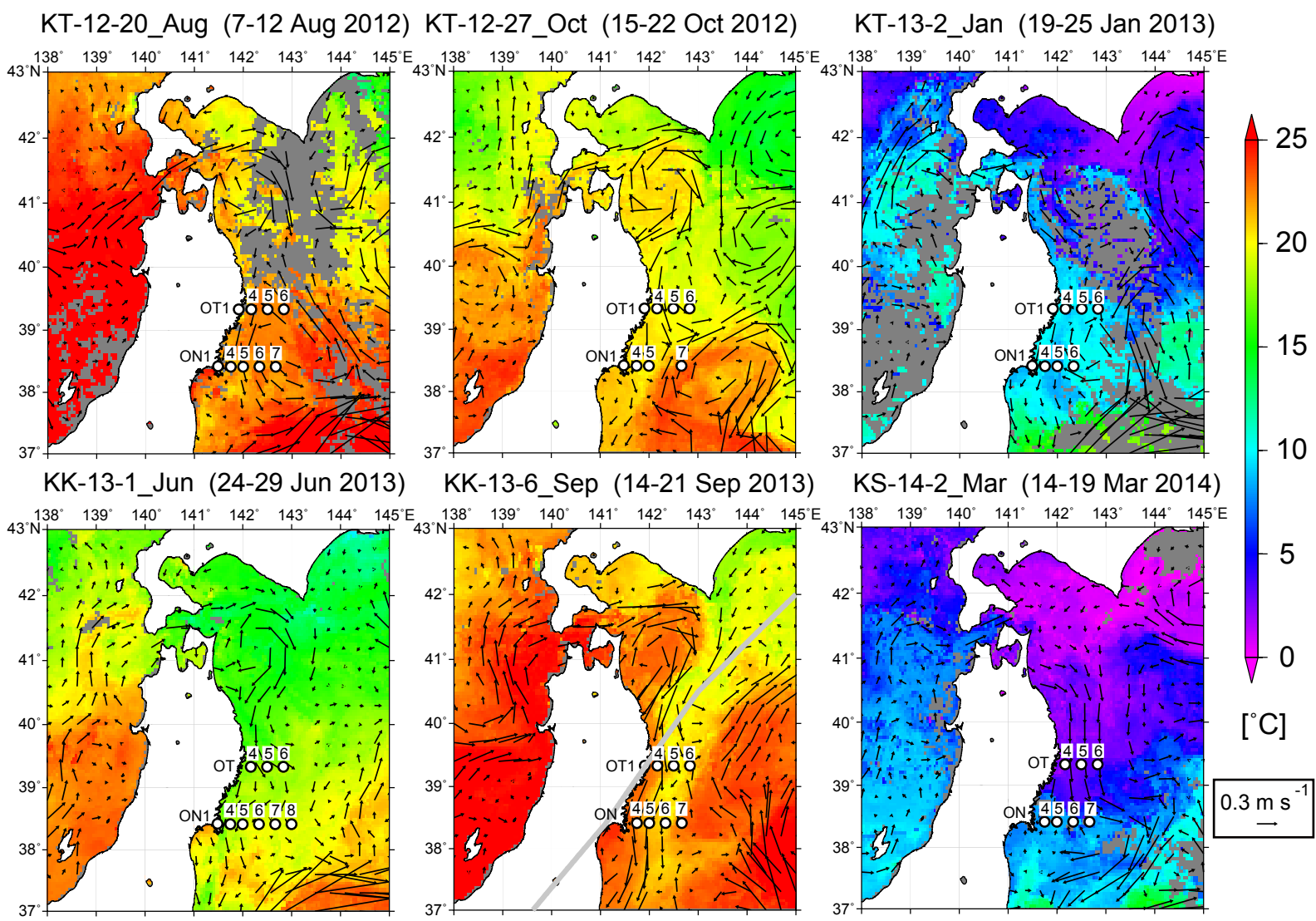


Fig S1 Shiozaki et al.

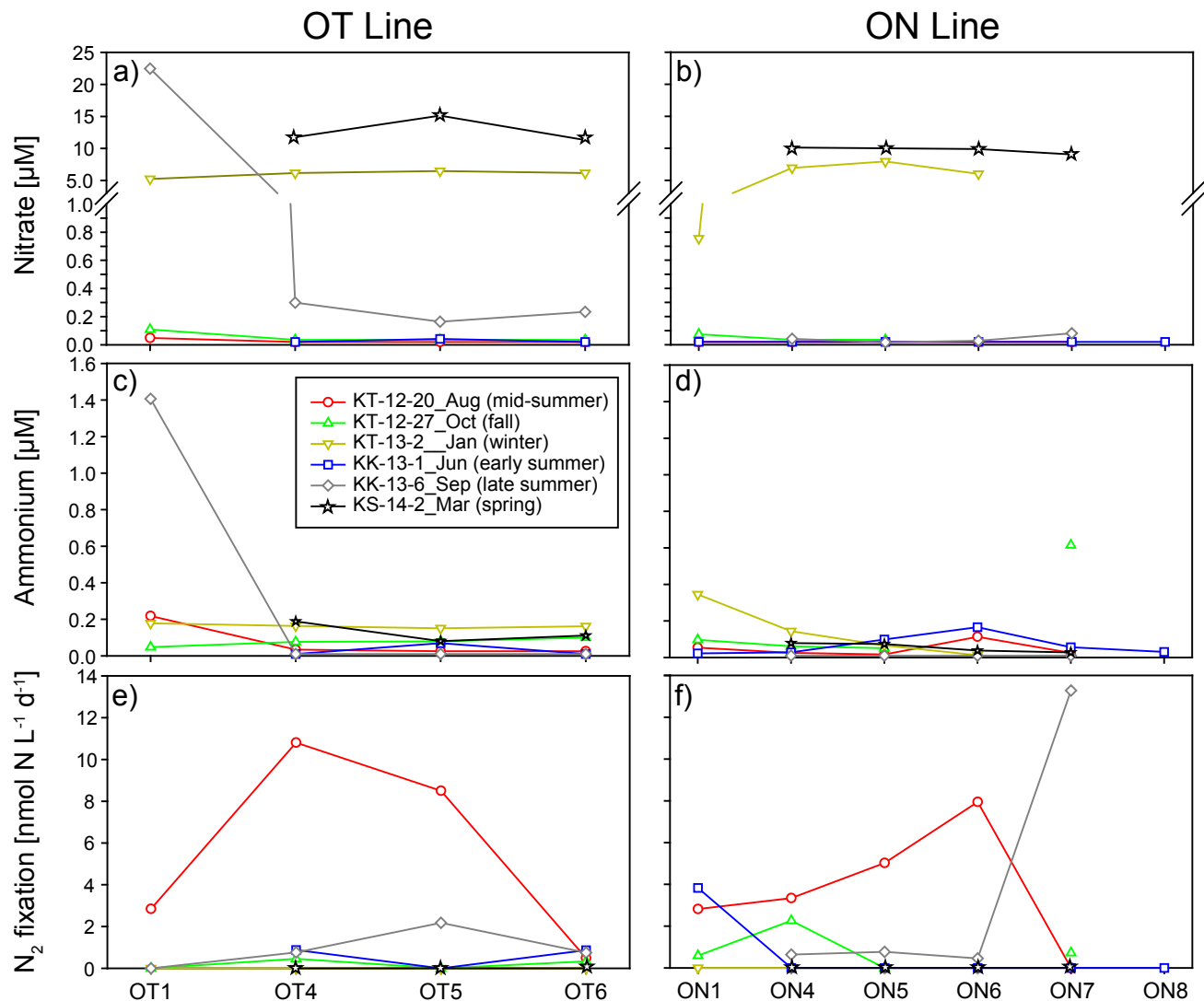


Fig S2 Shiozaki et al.

α -proteobacteria

β -proteobacteria

γ -proteobacteria

δ -proteobacteria

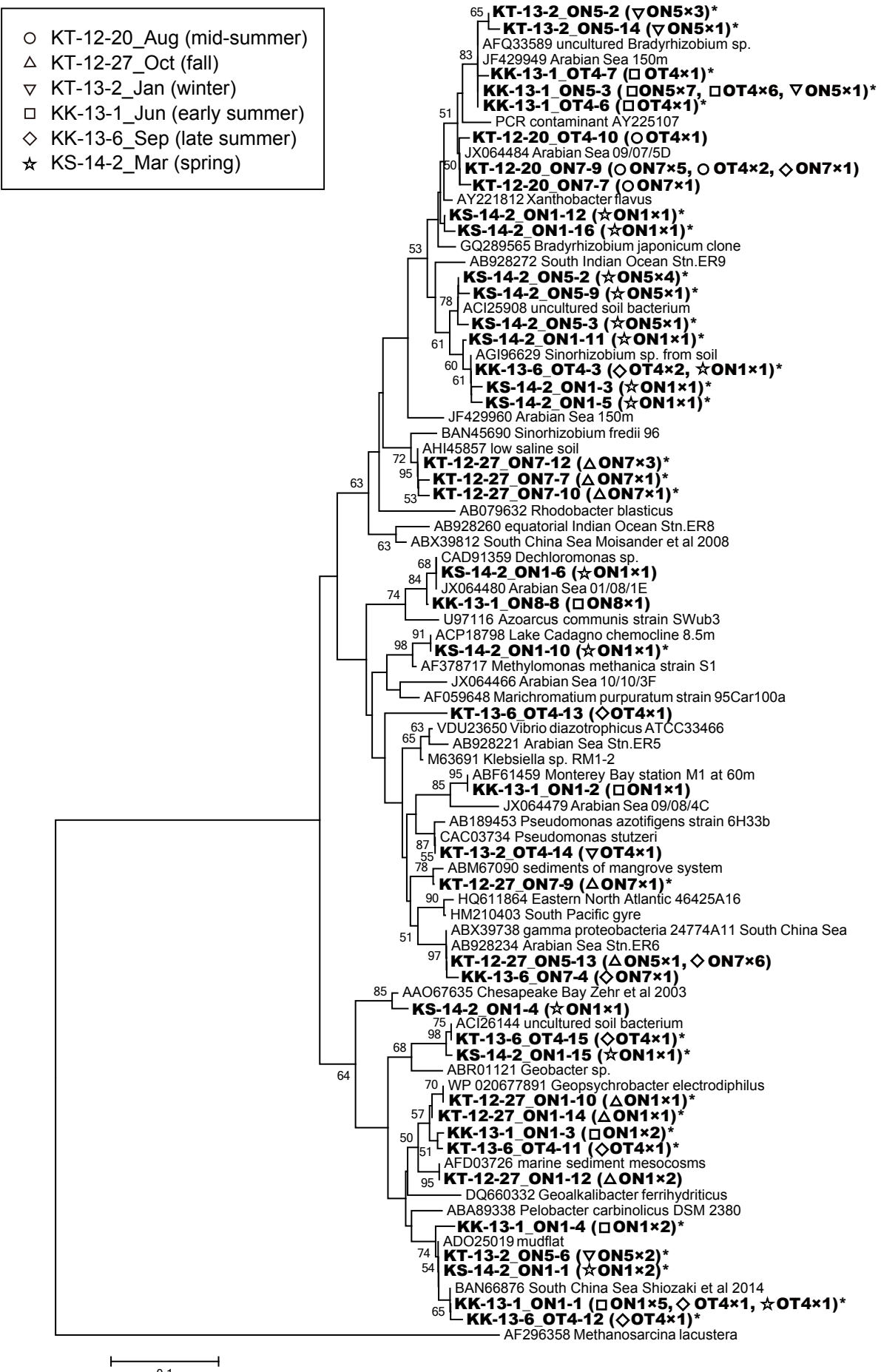


Fig S3 Shiozaki et al.

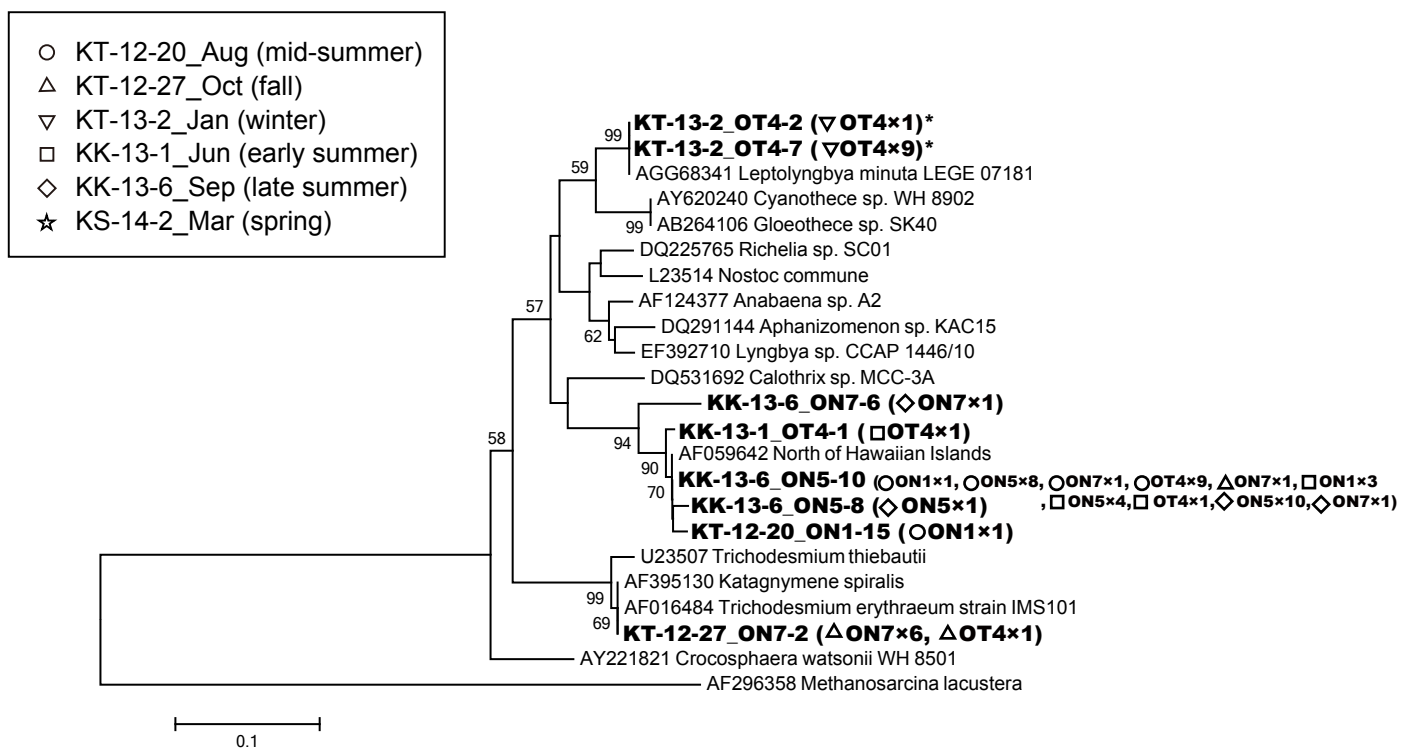


Fig S4 Shiozaki et al.

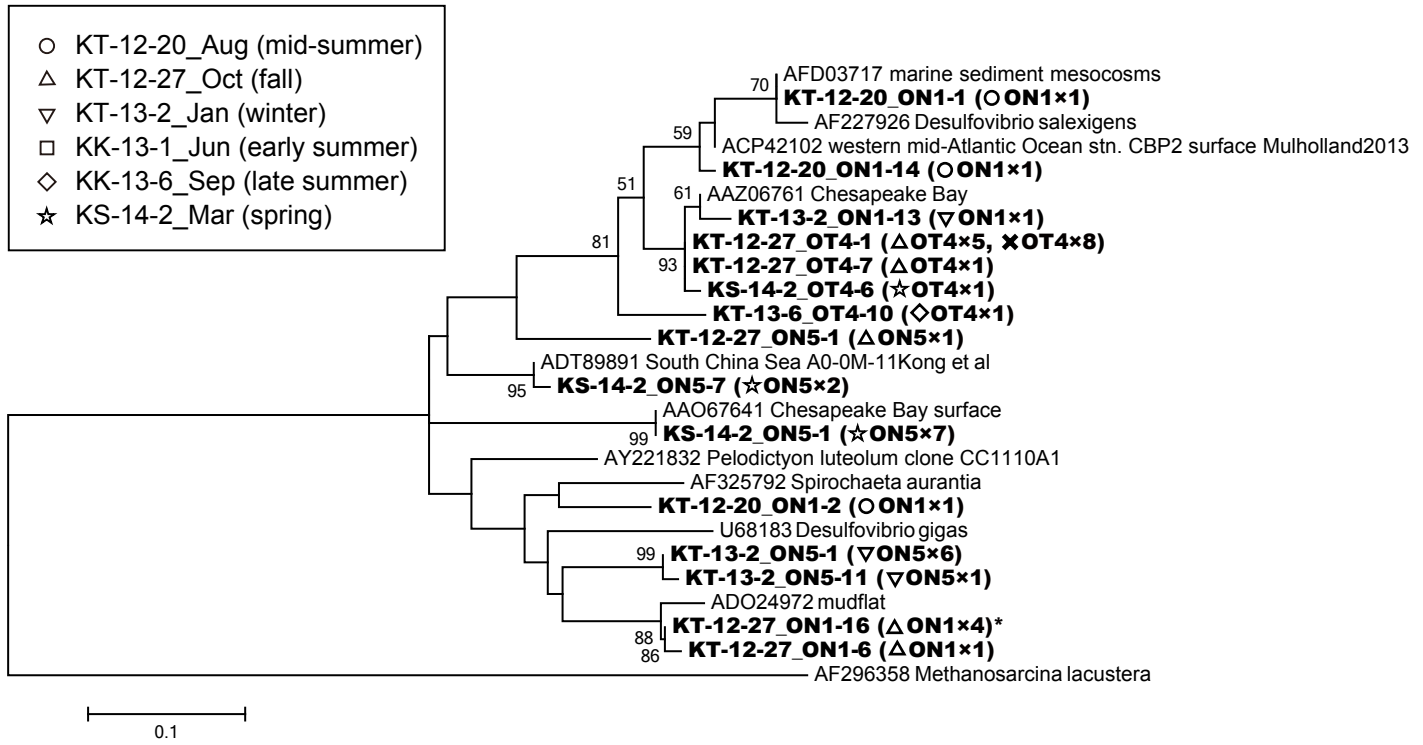


Fig S5 Shiozaki et al.

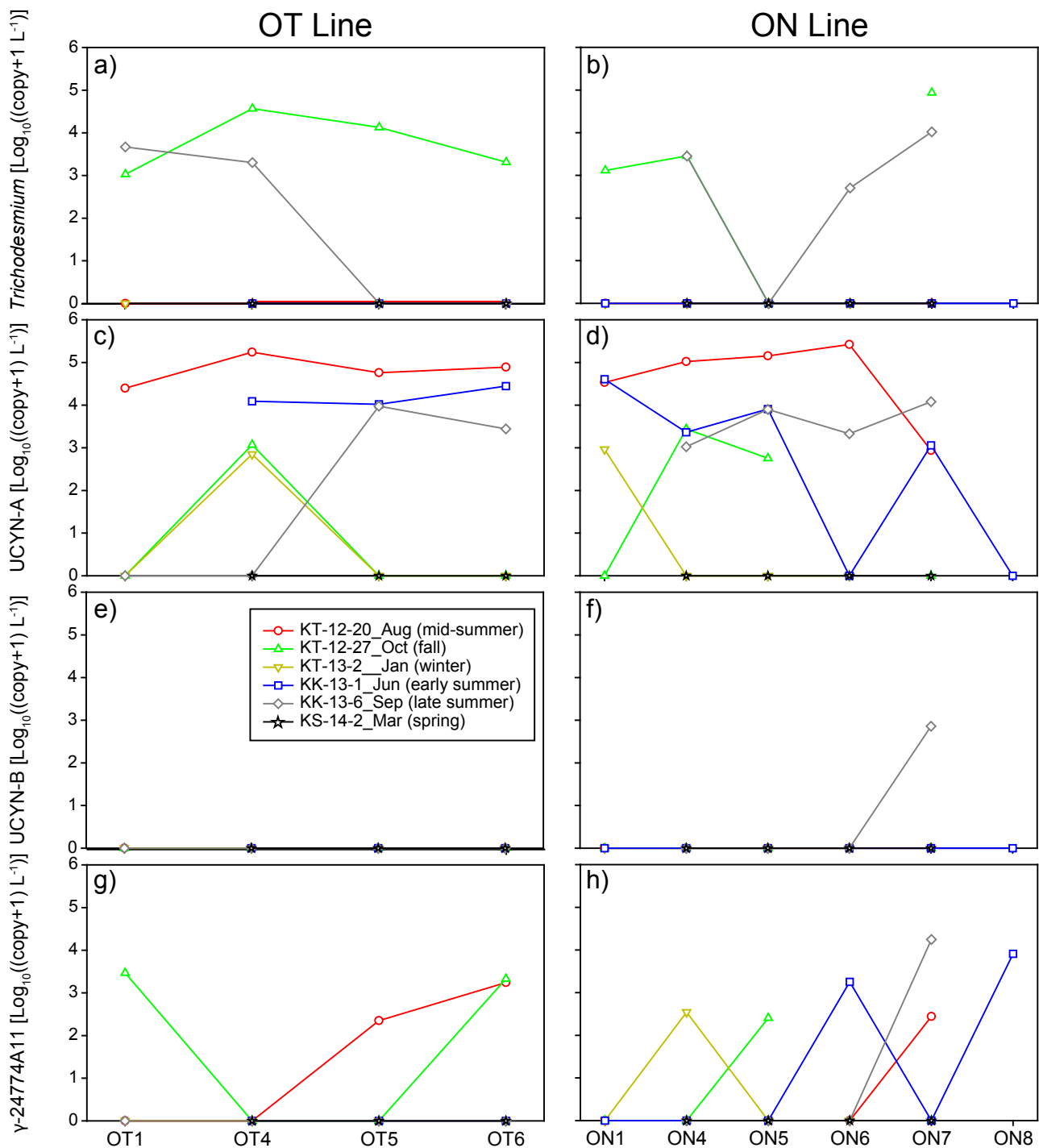


Fig S6 Shiozaki et al.

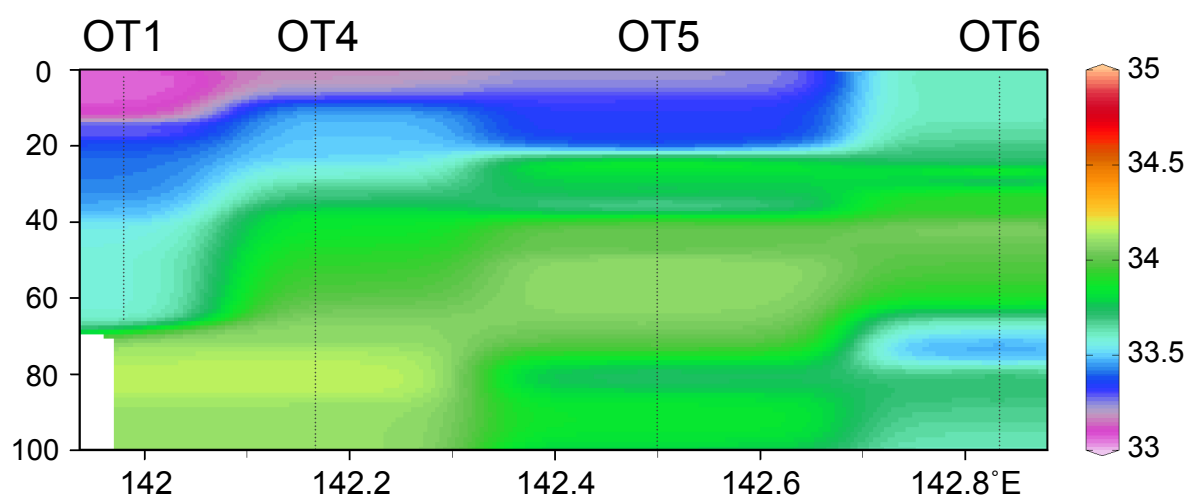


Fig S7 Shiozaki et al.

KT-12-20_Aug mid-summer KT-12-27_Oct fall KT-13-2_Jan winter KK-13-1_Jun early summer KK-13-6_Sep late summer KS-14-2_Mar spring

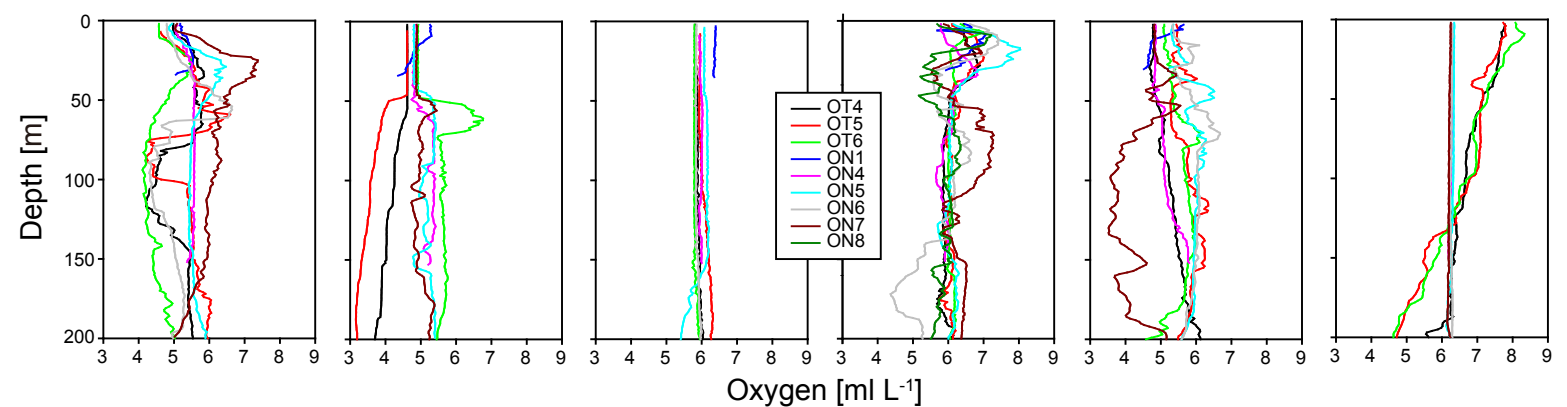


Fig S8 Shiozaki et al.